A CYTOPLASMIC ROLE FOR HISTONE METHYLTRANSFERASE (MET-2) IN *CAENORHABDITIS ELEGANS*

by

Ime Mimi Nkanta

A thesis submitted to the Faculty of the University of Delaware in partial fulfillment of the requirements for the degree of Master of Science in Biological Sciences

Spring 2022

A CYTOPLASMIC ROLE FOR HISTONE METHYLTRANSFERASE (MET-2)

IN CAENORHABDITIS ELEGANS

by

Ime Mimi Nkanta

Approved: ____

Jessica Tanis, Ph.D.
Professor in charge of thesis on behalf of the Advisory Committee

Approved: ____

Velia Fowler, Ph.D.
Chair of the Department of Biological Sciences

Approved: ____

John A. Pelesko, Ph.D.
Dean of the College of Arts and Sciences

Approved: ____

Louis F. Rossi, Ph.D.
Vice Provost for Graduate and Professional Education and
Dean of the Graduate College

ACKNOWLEDGMENTS

I would like to express my gratitude to Dr. Jessica Tanis for supporting, mentoring, and encouraging me over the last three years throughout my Graduate experience. Her teachings have made me a better student and increased my passion for research. I am so grateful to have had the chance to conduct research in your lab and for the lifelong friendships that this experience has helped me forge. I would like to appreciate my thesis committee members: Dr. Tanis, Dr. Fowler and Dr. Jaramillo-Lambert for all their support and encouragement throughout my graduate research and writing process. I would also like to thank the members of the Tanis Lab: Andy Lam, Rachael Gill, Michael Clupper, Malek Elsayyid, Denis Touroutine, Katherine Wagner, Erin Smith, Carter O'Brien, John Salsini-Tobias, Allison Davis, Emylee Kerslake, Karli Sunnergren and Juntian Wei for always helping me out and making me very happy to come into lab every day. Working with you all in lab has made my experience very wonderful and memorable. I would especially like to thank Andy Lam for being a great mentor to me when I first joined the lab, teaching me all the necessary lab techniques and always helping me out whenever I needed help. I would also like to thank Betty Cowgill because I wouldn't have been able to get to this point without your help. Thank you to the University of Delaware and the Biological Science department Graduate Program for giving me the opportunity and resources to conduct research and earn a Graduate degree. Finally, I would like to thank my friends and family who have supported, encouraged, and cheered me on throughout this journey.

TABLE OF CONTENTS

LIST OF FIGURES

ABSTRACT

Histone methyltransferases (HMTs) are known to affect chromatin condensation by methylating histones in the nucleus. Our collaborators from the Mango lab identified tropomyosin, which acts in the cytoplasm to regulate muscle contraction and stabilize actin filaments, as a potential target of the histone methyltransferase MET-2 through mass spectroscopy. We discovered that *met-2* mutant animals, *lev-11* knockdown animals, and animals expressing MET-2 with a nuclear localization sequence (NLS), all exhibited hypersensitivity to the acetylcholine receptor agonist levamisole. These results demonstrated that loss of *met-2* and tropomyosin cause the same phenotype, and suggest a cytoplasmic role for MET-2 since sequestration of this histone methyltransferase in the nucleus resulted in a phenotype indistinguishable from the mutant. *C. elegans* body wall muscles send out actin-rich projections called muscle arms which extend from the body-wall muscles to the nerve cord, allowing the muscle cell to be innervated. Tropomyosin mutants have fewer and wider muscle arms compared to wildtype. To investigate if the loss of *met-2* in the cytoplasm would also disrupt muscle arm morphology, I performed extensive imaging of muscle arms in wildtype, *met-2* mutants, and NLS::MET-2 animals using LSM880 confocal microscopy. I observed that *met-2* mutants exhibited significantly wider and more branched muscle arms compared to wild type but had no significant difference in the number of arms per muscle. This indicates that MET-2 function is necessary for proper muscle arm morphology but not for muscle arm formation. The NLS::MET-2 animals displayed muscle arm width and branching indistinguishable from wild type

animals, which suggests that MET-2 may affect the transcription of genes required to regulate the width of muscle arms. To determine if MET-2 localizes to the cytoplasm of the body wall muscles, I used the Andor Dragonfly spinning disk and super resolution microscope to visualize MET-2::GFP and observed cytoplasmic signal in a striated pattern in the body wall muscles. I am currently imaging a strain that expresses both MET-2::GFP and TOMM-20::DsRed2 to determine if the MET-2::GFP colocalizes with TOMM-20::DsRed2, a fluorescent protein used to visualize muscle mitochondria. In conclusion, I determined that loss of *met-2* leads to defects in muscle arm morphology. While NLS::MET-2 animals exhibit wild type muscle arm morphology, it remains unclear whether this is because MET-2 nuclear function impacts muscle arms or if NLS::MET-2 is not actually sequestered in the nucleus. However, my MET-2::GFP images showing cytoplasmic localization of a histone methyltransferase for the first time are consistent with a role for MET-2 in the cytoplasm.

Chapter 1

INTRODUCTION

1.1 Actin and Actin Regulating Proteins

Actin is present in both prokaryotic and eukaryotic cells. It is the most abundant protein in most eukaryotic cells and is responsible for essential processes including maintaining cell structure, transcription, cell division, motility, signaling, polarity, and muscle contraction. Actin can exist as G-actin (monomeric) and F-actin (filamentous), where the filamentous actin polymerizes at both ends by adding monomers (Carballido, 2006). F-actin goes through a process called treadmilling at a steady state where it loses subunits at the negative end (slow-growing end) and gains at the positive end (fast-growing end) (Carballido, 2006). It also makes up the complex and dynamic network of microfilaments, which have various functions and support the basic structure of eukaryotic cells. Microfilaments are made of double-stranded polymerized F actin that bind intracellularly with proteins like myosin to coordinate contraction enable cell motility. They are attached to the plasma membrane of cells to aid and modulate the tightness of tight junctions, secretion, endocytosis, exocytosis, and vesicle transfer. (Crawford et al, 2018).

Several actin-binding proteins play very key roles in many cellular functions. Aside from hydrolysis and nucleotide-binding, actin-binding proteins (ABPs) also regulate the polymerization of actin by their ability to nucleate, cleave, cross-link, destabilize and stabilize actin filaments (Dominguez and Holmes, 2011). Actin binding proteins can be classified into seven groups: 1) filament-depolymerizing proteins like cofilin that cause F-actin to be converted to G-actin, 2) monomer-binding proteins like thymosin that prevent the polymerization of G-actin, 3) filament severing proteins like gelsolin that bind to F-actin and cut it to reduce the length of the filament, 4) filament end-binding proteins like tropomodulin that prevent the exchange of monomers at the barbed end by capping the ends of the actin filament, 5) cross-linking proteins like Arp2/3 are responsible for branching of the filaments that results in 3D networks and filament bundling, 6) stabilizing proteins like tropomyosin that prevent depolymerization and stabilize actin filaments by binding tightly to the sides the filaments, and 7) motor proteins like myosin heavy chains (MyHCs) that use actin filaments. Some ABPs have multiple functions and can fall under more than one group (Dos Remedios et. al, 2003).

Actin in eukaryotes is grouped into three classes: α-, β-, and γ-isoforms that are mostly located in the cytoplasm but can also be found in the nucleus. The α- isoform is found in striated muscle cells like cardiac and skeletal muscle, while the β- and γ-isoforms are found in smooth and non-muscle cells (Dos Remedios et. al, 2003). Skeletal muscles which are responsible for voluntary movements have myofibrils in their cytoplasm which are cylindrical bundles that have thick filaments of myosin and thin filaments of actin. The myofibrils are arranged in stacked units called sarcomeres.

The end of each sarcomere is bounded by the Z disc, where the positive ends are at the outer ends and the negative ends are inwards towards the middle of the sarcomere. The thick filaments of myosin called the A band stretches across the center of the sarcomere towards the Z discs. The thick filaments are held together by a protein called myomesin also known as the M-line. The thin filaments of actin, also called the I-band extends inward toward the M-line into the A-band and form an overlap with the thick myosin bands. It is firmly anchored to the Z-discs by a protein called α-actinin and does not extend into the H-zone which only contains myosin.

Myosin has three regions, a tail, a neck-hinge, and a head which has actin and ATP binding sites. Actin on the thin filaments has a binding site for myosin, troponin, and tropomyosin. Tropomyosin wraps around the myosin binding sites on actin and is released when Ca^{2+} from the sarcoplasmic reticulum binds to the troponin C (TnC). Contraction in the muscles begins when the Z-discs moves together and the I-band and H-zone contract towards the A-band allowing for myosin to bind to actin in the absence of ATP. When ATP binds, the actin-myosin complex dissociates, and myosin undergoes a conformational change when the ATP hydrolysis (ADP and Pi). ADP and Pi stay attached to the myosin head and moves the myosin until it reattaches to a new position on the actin filament releasing ADP and Pi which pulls the actin filament forward toward the M-line. This motion is called the power stroke (Cooper, 2000). Muscle contraction and relaxation is mainly supported by the interaction of actin with myosin (Pollard and Cooper, 2009).

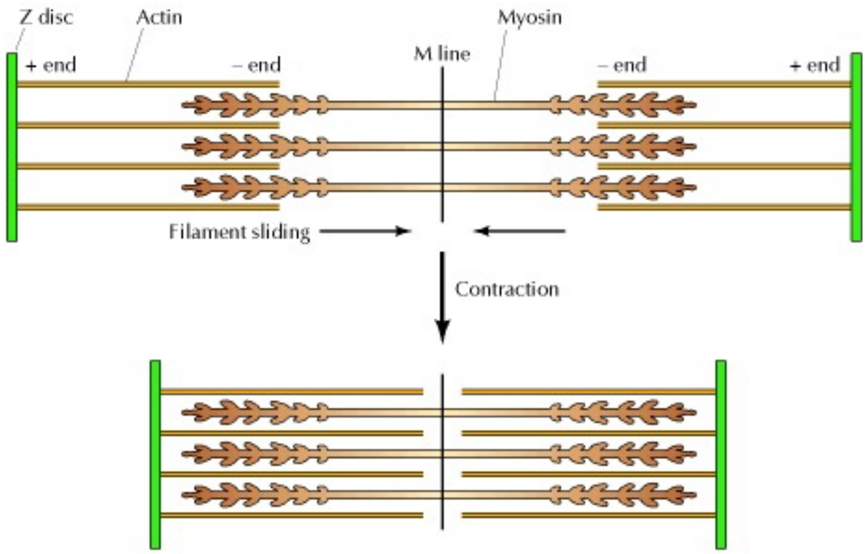

Figure 1: **Model of sliding-filament during muscle contraction** (Cooper GM, 2000). The actin filaments slide past the myosin filaments toward the middle of the sarcomere. This results in the shortening of the sarcomere without any change to the length of filament

1.2 Caenorhabditis elegans

C. elegans are very small, non-parasitic nematode worms that can be found worldwide in damp soil and sometimes in rotting vegetable material (Frezal & Felix, 2015). They breed in large sizes of 300 offspring per animal and have a very short life cycle, growing from egg to fertile adult in ~4 days (Frezal & Felix, 2015). The adult worms grow to a length of 1.3mm and a diameter of 80µm if they are well fed. Food source and temperature play a significant role in increasing or reducing the generation time of the worm. The wild-type strain, Bristol N2, has a lifecycle of 3.5 days to get to adulthood at 20°C. The same wild-type strain at 25°C becomes an adult in 3 days and at 15°C take a longer time of 4 days to get to adulthood (Brenner 1974). *C. elegans* are fed with OP50, a uracil requiring a mutant of *E. coli* that is seeded on nematode growth media (NGM) plates. The NGM has limited uracil, which prevents overgrowth of the OP50 bacterial lawn on the plates, which would hinder the visibility of the worms (Brenner 1974).

Wildtype *C. elegans* exist in two sexual forms: self-fertilizing hermaphrodites and males. The adult males have a copulatory bursa at the tip of their tail and appear to be smaller in size compared to hermaphrodites (Riddle et al, 1978). The hermaphrodites are different from the males in that they have two X chromosomes (XX) while the males have just one X chromosome (XO). They can reproduce either by males (XO) breeding with the hermaphrodites (XX) or by the self-fertilizing hermaphrodites. During hermaphrodite development, at the L4 stage, the gonad produces sperm that is stored in the spermatheca. When the worm gets closer to adulthood the germline then produces oocytes (Corsi et al, 2015). Mature self-fertilizing hermaphrodites can produce about 300 offspring that are fertilized by stored sperm while hermaphrodites that mate with males produce over 1200 offspring. Most of the offspring from the self-fertilizing hermaphrodites turn out to be hermaphrodites, and only about 0.1-0.2% turn out to be males due to the nondisjunction of the X chromosomes at meiosis. The majority of males are produced from the cross-fertilization of males and hermaphrodites. Moreover, heat shock can also be used to increase the number of males produced by a hermaphrodite progeny (Riddle et al, 1978).

There are four larval stages (L1-L4) in the development of a *C. elegans* embryo. The L1 stage lasts for 16 hours and the L2 to L4 stages lasts for 12 hours (Corsi et al, 2015). Newly hatched worms, under normal conditions, pass through all four larval stages and become mature adults after 3 days. During stressful conditions such as insufficient food, crowding, and heat, the animals can shift to an alternative developmental route and enter a pre Dauer stage (L2d), which is followed by the Dauer also known as the non-feeding diapause stage called Dauer (an alternative L3 stage). During the Dauer stage, a cuticle forms around the worm and plugs its mouth preventing it from eating and therefore halting development until conditions become favorable and the animal is able to feed again and develop into an adult. The cuticle that forms around the animal in the Dauer stage is resistant to various environmental stresses and chemicals for several weeks or months (Raizen et al, 2008).

C. elegans, for several reasons, has been a good model organism to study different systems and processes. A mature adult hermaphrodite has 959 somatic cells and a nervous system that is made up of about 302 neurons (Pathak et al, 2020). It is the only organism whose nervous system has been completely mapped and each neuron is different in properties, morphology, connectivity, and position. 38% of these protein-encoding genes in *C. elegans* have human orthologs, which can allow the study of various human diseases in *C. elegans* (Shaye and Greenwald 2011). Worms are optically transparent, which makes it easy to visualize their cells and subcellular details. Using fluorescent proteins to tag proteins helps to define subcellular localization of these proteins. Additionally, strains can be frozen for long periods of time for future experimental use.

Figure 2: Image of an adult hermaphrodite *C. elegans*.
C. elegans are a great model system for studying different cellular and molecular processes because they are simple, transparent, reproducible, genetically tractable, and have a short generation time.

1.3 Roles for Actin in C. elegans

Actin is very crucial to the fertility and development of *C. elegans*. An intact actin cytoskeleton is necessary for proper developmental patterning of the animal because once the one-cell embryo is fertilized, the actin cytoskeleton is needed for polarization and allows for the asymmetrical division of the embryo (Valarde et. al 2007). In a study done by Valarde et. al, they found that animals with depleted actin showed a drastic reduction of fertilized embryos as compared to the control animals that produced twice as long. Based on their study, they concluded that actin is required for proper oocyte development, cytokinesis, and chromosome segregation.

Other studies have also held actin responsible for different morphological changes that *C. elegans* experience in the different developmental stages including the projection of muscle arms from the body wall muscle to the nerve cord from embryogenesis to the larval stages. Adult *C. elegans* have 95 body wall muscles that are arranged in four quadrants along the total length of the animal and are necessary for movement. The two dorsal quadrants flank the dorsal cord, while the two ventral quadrants flank the ventral cord (Dixon and Roy 2005). The body wall muscles of nematodes send out actin-rich projections called muscle arms that make contact with the nerve cord allowing the muscle cell to be innervated (Sulston and Horvitz, 1977). Sixty-three body wall muscles project muscle arms to motoneurons on the nerve cord, sixteen anterior body wall muscles in the head project muscle arms to the nerve ring, and sixteen neck body wall muscles project muscle arms to both the nerve ring and the nerve cord. Synapses form where the muscle arms contact the nerve cord (Dixon and Roy 2005).

The development and extension of muscle arms towards the nerve cord remains is not completely understood, but their extension is thought to be guided by a chemoattractant. The growth of muscle arms is regulated differently during embryogenesis and the larval stages in *C. elegans*. The development of the first muscle arms starts during embryogenesis when the myoblasts move away from the nerve cord (Dixon 2006). As the myoblast moves away, it leaves muscle membrane behind still attached to the nerve cord, resulting in muscle arm formation. The number of muscle arms per body wall muscle varies in each stage of the animal's life cycle.

There is an average of 1.7 muscle arms per body wall muscle on newly hatched animals. At the second larval stage (L2), there is an average of 3.4 muscle arms per body wall muscle and by the time the animal gets to adulthood, each body wall muscle has an average of 4.0±1.0 muscle arms (Dixon and Roy 2005).

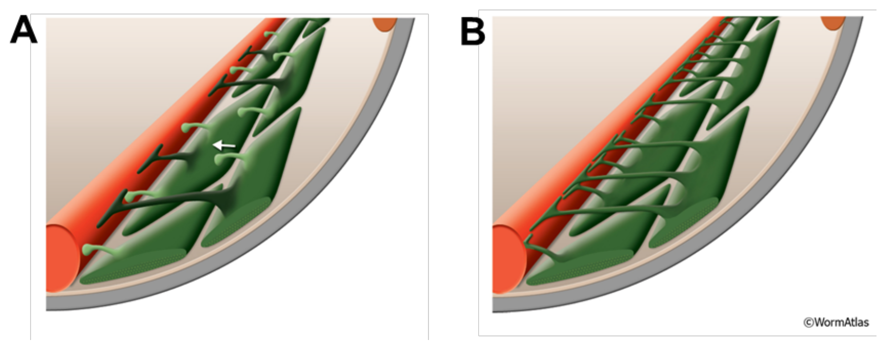

Figure 3: **Muscle Arm Development in *C. elegans*** (Altun and Hall, 2005). (A) During embryogenesis, the myoblast moves away from the motor neuron and leaves behind one or two muscle arms (dark green arm extensions). Occurs during larval stages, where additional muscle arms grow from the body wall muscles to the nerve cord (light green arm extensions). (B) Adult animals have roughly three to six body wall muscles.

1.4 Neuromuscular Junction

The neuromuscular junction (NMJ) is a specialized chemical synapse between a motor neuron and a muscle fiber. At the NMJ, motor neurons to transmit signals to the muscle fiber, causing muscle contraction. The nervous system works hand in hand with the muscles because the muscles have to be innervated to function and support movement (Rygiel, 2016). At the NMJ, synaptic transmission begins at the presynaptic terminal of a motor neuron. Acetylcholine (ACh), a neurotransmitter is loaded into the synaptic vesicle by the vesicular acetylcholine transporter (VAChT). When the neuron undergoes depolarization, voltage-gated calcium (Ca^{2+}) channels that allow calcium ion (Ca^{2+}) to enter the neuron are activated (Levitan et al. 2015). The calcium ions (Ca^{2+}) bind to synaptotagmin, a sensor protein on the synaptic vesicle that causes the vesicles to fuse with the cell membrane releasing acetylcholine (ACh) into the synaptic cleft (Levitan et al. 2015). The ACh released from the motor neuron diffuses across the synaptic cleft and binds to acetylcholine receptors (AChRs) on the cell membrane of the muscle cell. The AChRs open allowing sodium (Na^{+}) to flow into the muscle cell and causing it to depolarize. The depolarization of the muscle cell activates the ryanodine receptor, which allows calcium ions (Ca^{2+}) to flow out of the sarcoplasmic reticulum into the cytoplasm of the muscle. The Ca^{2+} binds to troponin C, which causes tropomyosin to move away from actin filament and allows myosin to bind for muscle contraction (McIntire et al. 1993).

C. elegans have motor neurons that are specialized to control forward and backward movements. The motor neurons are B-type, A-type and D-type. The B-type neurons are for forward movements and A-type neurons are for backward movement. The A and B-type motor neurons release acetylcholine (ACh) and form a synapse at the NMJ to innervate one side of the body wall muscles. The nicotine-sensitive acetylcholine receptor ACR-16 (nAChRs) is activated by nicotine and levamisole-sensitive acetylcholine receptors (L-AChRs) are activated by levamisole. Both types of acetylcholine receptors are expressed on the body wall muscles in the animal (Richmond and Jorgensen 1999). The D-type motor neurons inhibit the contralateral body wall muscles through GABAergic signaling. Thus, in *C. elegans* the body wall muscles receive both excitatory and inhibitory inputs from cholinergic and GABAergic motor neurons respectively. The wave-like locomotion of the worm results from an excitatory cholinergic signal on one side of the worm simultaneous to an inhibitory GABAergic signal on the opposite side of the body (Zhen and Samuel 2015).

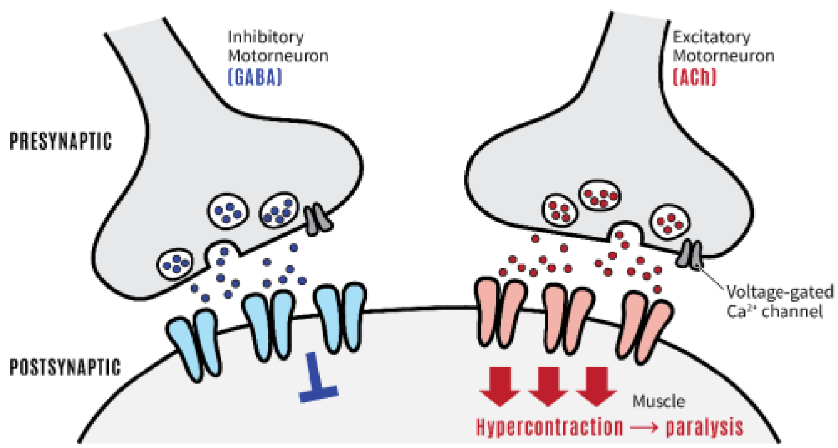

Figure 4: **The Neuromuscular Junction and effect of levamisole on *C. elegans*** (Hung et al, 2017). Muscle contraction occurs when ACh is released from motor neurons, diffuses across the synaptic cleft, and binds to acetylcholine receptors (AChRs) on the cell membrane of the muscle cell. Levamisole leads to hypercontraction and paralysis. It is a L-AChR agonist that causes activation of L-AChR. The release of GABA from inhibitory motor neurons leads to muscle relaxation.

1.5 LEV-11 (Tropomyosin)

Tropomyosin is one of the major actin filaments–binding proteins that regulate actin-myosin interaction and actin-filament stability. It is a rod-like coiled dimer that is bound to actin filaments in the cytoplasm and plays a central role in the calcium-dependent regulation of muscle contraction and cytoskeletal dynamics (Gateva et al. 2017). Tropomyosin binds to F-actin which significantly reduces the surface area on the actin filaments and blocks myosin-binding sites for the binding of myosin which regulates the muscle contraction (Manstein et al. 2016). In striated muscles, tropomyosin is part of the troponin complex and undergoes a conformational change when calcium (Ca^{2+}) binds to the troponin complex on the C site. This conformational change affects the positioning of tropomyosin on the F-actin and causes it to pull away from the actin exposing the active binding sites that allows myosin to bind to the filament and contraction to begin (Barnes et al, 2018). In non-muscle cells, tropomyosin is involved in muscle actin filament organization, cell migration, cytokinesis, and morphogenesis (Gunning et al. 2005).

Organisms have different tropomyosin genes that produce several isoforms. The diversity of tropomyosin isoforms stems from the constant changes and the complexity of the cells and tissues of organisms (Gunning et al. 2005). Although the functions and identity of many tropomyosin isoforms are still unknown, mammals have four tropomyosin genes that produce about 40 isoforms. The isoforms are located in different subcellular regions and play different roles in cells like organizing stress fibers, influencing neuronal cell morphology, and muscle contraction (Gallant et al.

2011). The budding yeast *Saccharomyces cerevisiae* has two tropomyosin isoforms from different genes that have different effects on the interaction between actin-myosin and the function of formin (Barnes et al, 2018). Recently, studies revealed a new tropomyosin isoform in *Drosophila* that plays important roles in mitotic spindles, microtubule-dependent mRNA localization, and intermediate filament-like cytoskeletal functioning (Goins and Mullins, 2015; Cho *et al.* 2016).

C. elegans has one gene for tropomyosin called *lev-11. lev-11* in mammals has been known to produce five isoforms through the utilization of two separate promoters and alternative splicing lev-*11* mutants were isolated from a screen that was performed for levamisole-resistant strains (Lewis *et al.* 1980). Levamisole acts as a nicotinic acetylcholine (ACh) receptor agonist that activates ligand-gated AchR on muscle cell membranes, allowing a steady influx of calcium (Ca^{2+}) which induces continued stimulation, contraction of muscles, and eventually leads to paralysis and immobilization in wild-type worms. Reduced levels of *lev-11* lead to hypersensitivity to levamisole-induced paralysis, while the hypermorphic alleles identified in the Lewis et al screen cause resistance. In the body wall muscle of an adult worm, *lev-11* is also involved in muscle arm extension, and muscle arm formation (Dixon and Roy, 2005). Reduction of LEV-11 function results in paralysis and complete loss causes lethality. *lev-11* also plays an important role in the reproductive system of the worm by regulating the contractility of male sex muscle and hermaphroditic gonadal myoepithelial sheath (Gruninger *et al.*2006; Ono and Ono, 2004).

1.6 Histone Methyltransferase

Histones are essential proteins found in the nucleus of organisms and form nucleosomes when DNA material is packaged into them. The nucleosome is made up of 8 histone proteins, 2 H2A, 2 H2B, 2 H3, 2 H4, and wrapped with 145 base pairs of DNA (Yang et al. 2020). Histones have lysine and arginine-rich N-terminal tails that make them subject to various covalent modifications like methylation, phosphorylation, and acetylation that can affect gene expression. These modifications can function either individually or in combination by modifying the affinity of histones to the negatively charged backbone of DNA. Thus, these modifications impact the structure of the chromatin and the regulation of gene expression (Casciello et al. 2015).

Histone methyltransferases (HMTs) are histone-modifying enzymes that catalyze the transfer of methyl groups to lysine and arginine residues of histone proteins. Methyl groups are attached at specific lysine and arginine residues on histones H3 and H4. Methylation of histones by HMTs is usually associated with gene silencing but the methylation of some residues like H3K4, H3K36, and H3K79 has been seen to cause gene activation (*Black et al. 2012*). Lysines can be monomethylated, dimethylated, and trimethylated while arginines can only be monomethylated and dimethylated. There are two main types of HMTs, the lysine-specific which can exist as SET domain-containing and non-SET domain-containing and arginine specific. A SET domain is a protein domain that possesses methyltransferase activity. The SET domain-containing HMT targets the lysine tail for methylation to occur and the non-SET domain-containing HMT uses an enzyme called Dot1 to methylate a lysine residue in the globular core of the histone (*Wood et al. 2004*). Arginine-specific HMTs are classified into three types of protein arginine methyltransferases (PRMTs). All three PRMTs methylate arginine residues on histone tails and produce either monomethylated arginine or symmetric dimethylarginine (Branscombe et al. 2001). Altered levels or activity of methylation-regulating enzymes like HMT can result in certain abnormal activities that contribute to various diseases like cancer, inflammatory diseases, infectious diseases, metabolic diseases, and some neurological diseases. Additionally, methylation can be reversed by histone demethylase which is an enzyme that removes methyl groups from histone proteins (Jambhekar et al. 2019). Most of the research done in the discovery of histone modification show that they play a role in the maintaining certain transcriptional memories.

In *C. elegans*, MET 2 is a histone methyltransferase that is required for the placement and accumulation of the repressive histone modification H3K9me2 in the adult germ line (Greer et. al, 2014). MET-2 encodes the ortholog of mammalian protein SetDB1, a H3K9 histone methyltransferase that supports transcriptional dormancy in embryonic stem cells (Checchi et. al, 2014). Furthermore, studies suggest that *met-2* plays an important role in ensuring that chromosomes undergo proper segregation during meiosis. During meiosis in male worms, MET-2-dependent H3K9me2 shields the unpaired X chromosome from being recognized versus asynapsed homologous chromosomes with respect to both checkpoint signaling and transcriptional silencing (Kerr et. al, 2014).

Our lab is collaborating with the Mango lab. They sought to identify proteins that were specifically methylated by MET-2 in *C. elegans*. To achieve this, they performed a pull-down with a lysine mono-methyl-specific antibody called Kme and used the mass spectrometer to identify the proteins were present in the wild type, but not the MET-2 sample. One of the proteins identified that was methylated in wild type but not in MET-2 animals was LEV-11. This was surprising because LEV-11 tropomyosin is a protein that is known to function in the cytoplasm to regulate muscle contraction and stabilize actin filaments.

1.7 Aims and Hypothesis

Based on the pull down, we hypothesized that MET-2 also has a cytoplasmic function and methylates LEV-11 in the cytoplasm. To test if MET-2 could have a cytoplasmic function our lab performed a series of sixty-minute levamisole time course behavioral assays to determine if knockdown of *lev-11* and *met-2* mutants have similar phenotypes. The results of the assay showed that the *lev-11* RNAi animals were more sensitive to levamisole compared to the wild type animals on empty vector (Figure 5). A similar result was also observed for *met-2* mutant animals, as they also showed hypersensitivity to levamisole compared to the wild type animals (Figure 6).

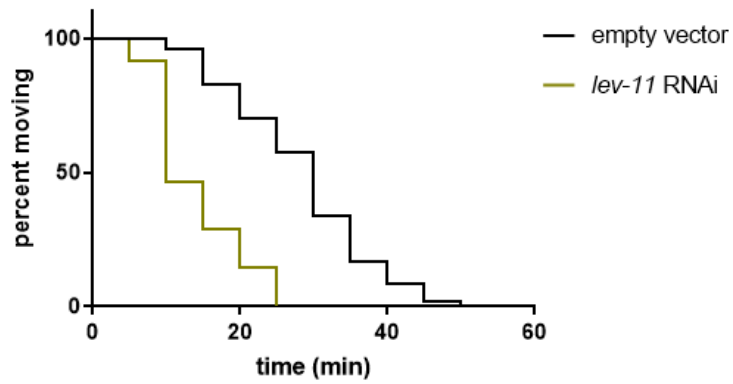

Figure 5: **Loss of *lev-11*(tropomyosin) Results in Levamisole Hypersensitivity.** Knockdown of *lev-11* (tropomyosin) (green, $p<0.0001$) resulted in levamisole hypersensitivity when compared to wild type on empty vector (black).

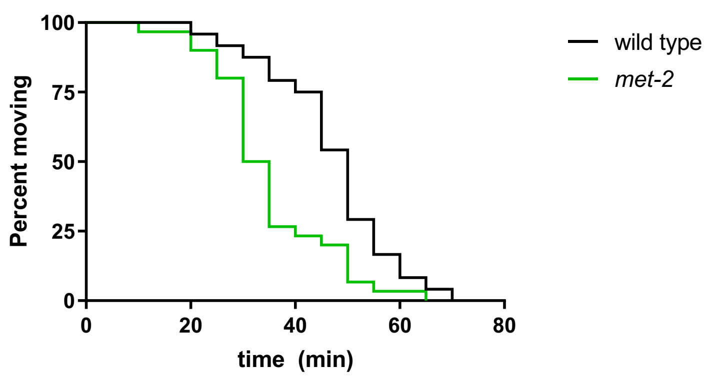

Figure 6: **Knockout of *met-2* Results in Levamisole Hypersensitivity.** *met-2* mutant animals (green, $p<0.0001$) paralyzed significantly faster than wildtype (black) indicating hypersensitivity to levamisole

We performed another sixty-minute levamisole time course assay with animals in which a nuclear localization sequence (NLS) had been inserted at the *met-2* locus using CRISPR. The NLS::MET-2 is fully functional, but due to the NLS, it is only present in the nucleus. The NLS::MET-2 animals also exhibited hypersensitivity, paralyzing before the wild type animals. The similarity in levamisole hypersensitive phenotype observed in the *lev-11* RNAi, and *met-2* mutant, and NLS::MET-2 animals suggests that MET-2 may play a cytoplasmic role.

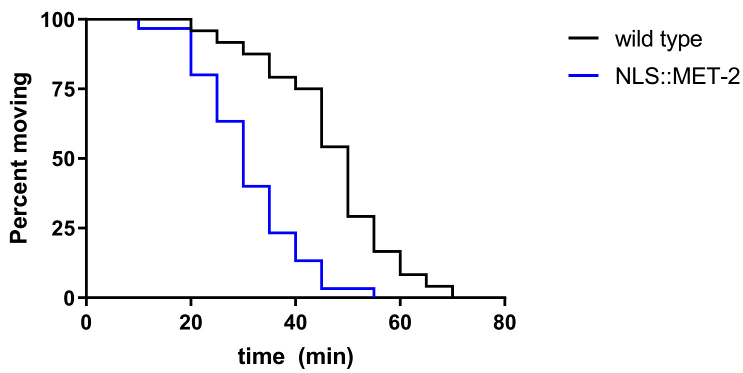

Figure 7: Sequestration of MET-2 in the Nucleus Results in Levamisole Hypersensitivity. Animals expressing MET-2 with a NLS (blue) exhibited levamisole hypersensitivity when compared to wildtype (black, $p<0.0001$)

I hypothesized that muscle arms could be disrupted by loss of *met-2* in the cytoplasm, as observed with loss of *lev-11,* and that this disruption of the NMJ could result in the observed levamisole phenotypes. My first aim was to image muscle arms in wild type, *met-2* mutant, and NLS::MET-2 animals expressing the *trIs30* transgene to visualize the muscle arms to determine if cytoplasmic MET-2 was required for proper muscle morphology. My second aim was to determine if MET-2::GFP does indeed localize to the cytoplasm of the body wall muscles.

Chapter 2

METHODS

2.1 Maintaining Strains

C. elegans are maintained on nematode growth media (NGM) plates. Media is made with 3 g NaCl, 2.5g peptone, and 17 g agar mixed into 1 L of distilled water. The mixture is autoclaved and allowed to cool to approximately 72°C for about an hour. While cooling, a stir rod mixes the media at moderate speed and the following additives are added: 1 mL cholesterol in ethanol (5 mg/mL), 1 mL 1M CaCl, 1 mL 1M MgSO, and 25 mL 1M potassium phosphate buffer (KH_2PO_4; pH 6.0). 10 mL of the media is pipetted per 6cm petri dish and 4 mL of the media is pipetted per 3cm (used mostly for crosses) petri dish. The plates are left to dry for about 2-3 days then the 6cm plates are seeded with 200 µL of OP50 and the 3cm plates are seeded with 100 µL of OP50, an E. coli strain, grown in B Broth (bactotryptone, NaCl and distilled water). The worms are maintained every 3-4 days when an old plate is overpopulated and running out of food (OP50). A flattened platinum wire is used to pick 3 hermaphrodite worms in L4 stage onto a new plate for the animals to continue breeding and have sufficient food. The NGM plates can also be used to grow a strain that has been frozen down. The frozen strain is left to thaw and then pipetted onto 4 seeded NGM plates. When maintaining or growing a new strain each new plate must be labeled accurately with the name of the strain, date, and stored 15°C or 20°C.

2.2 Creating Strains

In order to analyze muscle arms in animals that only have functional MET-2 in the nucleus, but not in the cytoplasm I had to first create the strain that will have functional MET-2 only in the nucleus. To create the strain, 6 wild-type males were crossed with 3 hermaphrodite RP247 animals that contain an integrated transgene (*trIs30*) that expresses YFP in the body wall muscles. From the progeny of the cross (F1 generation), I crossed 6 males with 3 hermaphrodites from the strain of worms that have MET-2 only in the nucleus (NLS::FLAG::MET-2) . After 4 days, I screened the F2 generation for YFP positive worms. I picked 5 YFP positive L4 worms and placed one worm per plate to self-fertilize and produce progeny. I screened the progeny produced in all 5 plates (F3 generation) and picked 24 worms that were YFP positive, placing one worm per plate to self-produce. After 3 days, I screened all 24 plates for plates that had 100% of its progeny to be YFP positive. The animals from the 100% YFP positive plates were lysed and genotyped to identify a plate that had a homozygous genotype for *trIs30;* NLS::FLAG::*met-2.*

In order to determine if MET-2::GFP localizes in the cytoplasm of the muscle and confirm that the expression of MET-2::GFP in not mitochondrial, I had to create a strain that expresses both MET-2::GFP and TOMM-20::DsRed2, which is a mitochondrial marker. To create the strain, SJZ47, which contains the TOMM-20::DsRed2 transgene *foxSi16* was heat shocked by puting 6 L4 hermaphrodite worms on 6 NGM seeded plates each and placing the plates in a 30^{o}C incubator for 6 hours. After the 6 hours the plates were then transferred and incubated at 20^{o}C. After 4 days, the heat shocked worms produced males. Four SJZ47 males were crossed with two MET-2::GFP hermaphrodites that express MET-2::GFP in the muscles. The progeny of the cross (F1 generation), was screened for RFP positive L4 hermaphrodites. The RFP positive L4 hermaphrodites were picked unto 5 plates, 1 worm per plate to self-fertilize and produce progeny. The progeny in all 5 plates (F2 generation) were screened and 24 L4 worms that were RFP positive were put in 24 plates; 1 worm per plate to self-produce. After 3 days, all 24 plates were screened for plates that had 100% of its progeny to be RFP positive. The animals from the 100% RFP positive plates were imaged on the Zeiss Observer microscope to determine which plates were homozygous for MET-2::GFP.

2.3 Preparing Strains for Imaging

In preparing strains, it is important that the worms are imaged in adulthood so about 30 animals in the L4 stage were picked from each strain unto new plates 24 hours before imaging. The strains used were RP247 *trls30* animals to image muscle arm in wild type animals, *trls30*; *met-2* animals to image muscle arms in the HMT mutant, and *trls30*; NLS::FLAG::MET-2 to image muscle arms in animals that have MET-2 in the nucleus but not in the cytoplasm. MET-2::GFP animals used to determine the localization pattern of MET-2 in the muscle cytoplasm. Before imaging, a 3% agar pad was prepared on a slide, 5µL of 10mM levamisole was placed unto the agar and about 8 to 10 animals from each strain were immobilized with the levamisole.

2.4 Rolling worms for imaging muscle arms

The only way muscle arms can be properly seen is when the worm is rolled such that the vulva is facing either up or down and not to the side. The rolling of the animal is important to ensure a proper orientation for imaging. To roll the animal, a worm pick is used to pick the desired number of worms to be imaged unto a slide with levamisole. Then the worm pick is used to vigorously whisk the worms on the slide for about 40 seconds. Lastly, a coverslip is then placed on the top of the slide.

2.5 Confocal Microscopy

A Zeiss LSM880 Confocal Microscope was used to image muscle arms. As mentioned above, *trls30* and *trls30*; *met-2* animals grown on OP50 and were used as controls to visualize the muscle arm phenotype. All images were taken in short Z-stacks with a step size of .19 microns with the following parameters: averaging of 2, 12-bit depth, 2032 frame size, 514 nm argon laser, gain of 792, digital offset of 0, and digital gain of 1. The Z-stacks were obtained using a 40x water objective. For the *trIs30* transgene, DsRed2 is expressed in the nerve cord and YFP in the muscle and muscle arms. As there is spectral overlap between YFP and DsRed2, the images had to be spectrally unmixed. Spectral unmixing is used in multi-color fluorescence labeling to distinguish between the colors, untangle fluorescence spectral overlap and reduce the possibility of bleed through within channels. Maximum intensity projections of Z-stacks were processed and then those images were used for analysis.

2.6 Image Analysis

All the images were analyzed with Zen Blue and muscle arms were counted per muscle manually by eye. Each muscle arm was measured by width in nanometers (nm) using the ruler tool in Zen Blue. All muscle arms were measured for muscle arm width at the thinnest point, including the muscle arms that branch off the main muscle arm migrating towards the nerve cord. The width of all muscle arms was recorded in an excel spread sheet and the average muscle arm width per muscle was calculated. Welch's two-tailed t-tests with unequal variance were used to test significance for both muscle arm number and muscle arm width. All values from the analysis were entered into Graph Pad Prism and corresponding graphs were generated.

Chapter 3

RESULTS

3.1 Analysis of Muscle Arms in Wild-type and *met-2* mutant *C. elegans*

C. elegans body wall muscles send out actin-rich projections called muscle arms which extend from the body-wall muscles to the nerve cord. Muscle arms make up the postsynaptic region of the neuromuscular junction (NMJ) allowing the muscle cell to be innervated (Dixon and Roy 2005). Dixon and Roy showed that *lev-11* (tropomyosin) knockdown animals exhibit significantly wider and fewer muscle arms compared to wildtype animals (Dixon and Roy 2005; Figure 8). Erin Smith, an undergraduate student in our lab was able to replicate these findings by using RNAi to knockdown tropomyosin, observing a similar phenotype of fewer and wider muscle arms (data not shown).

To determine if the *met-2* mutants also display a muscle arm phenotype, Erin performed imaging of *met-2* mutant and wild type animals using LSM880 confocal microscopy. The images were analyzed by measuring each muscle arm at the thinnest point (Figure 9 A, B). Her results showed that *met-2* mutant animals exhibited significantly wider muscle arms ($p< 0.05$) compared to wildtype and wildtype animals also displayed a higher number of muscle arms per muscle ($p<0.05$) compared to the *met-2* animals (Figure 10).

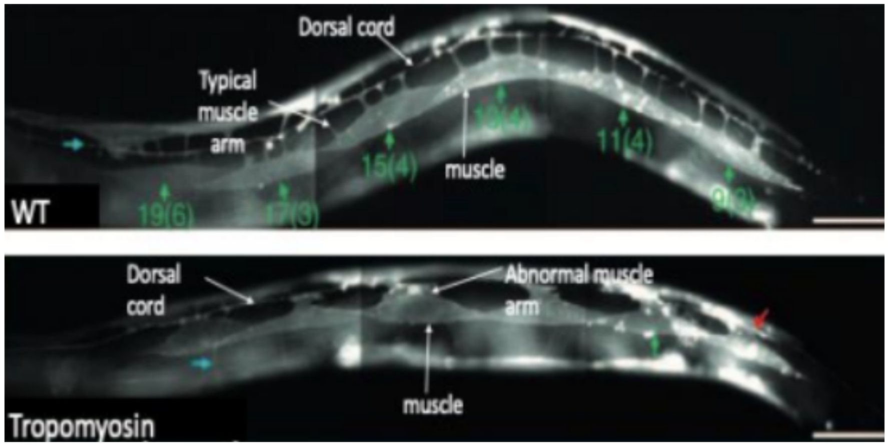

Figure 8: ***lev-11*(tropomyosin) Knockdown Causes Wider and Fewer Muscle Arms** (Dixon and Roy 2005). Wild-type animals have 3 to 4 very thin muscle arms per muscle while the *lev-11* (tropomyosin) knockdown has about 1 or 2 very thick muscle arm per muscle.

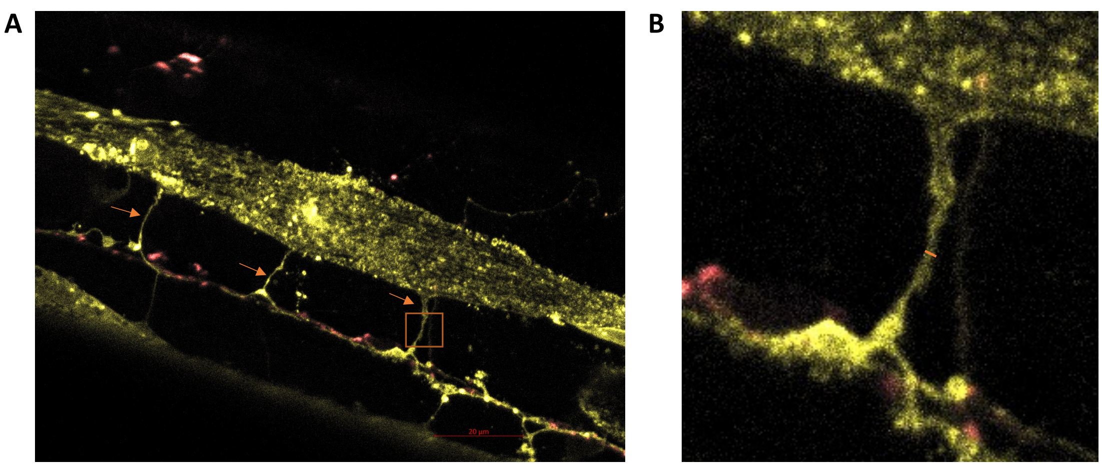

Figure 9: **Muscle Arm Visualization in Wildtype.** (A) Confocal image of wildtype with the dorsal nerve cord (red), muscles and muscle arms (yellow). Muscle arms are indicated with orange arrows and orange box shows muscle arm thinnest point. (B) Muscle arm is measured at the thinnest point (orange line).

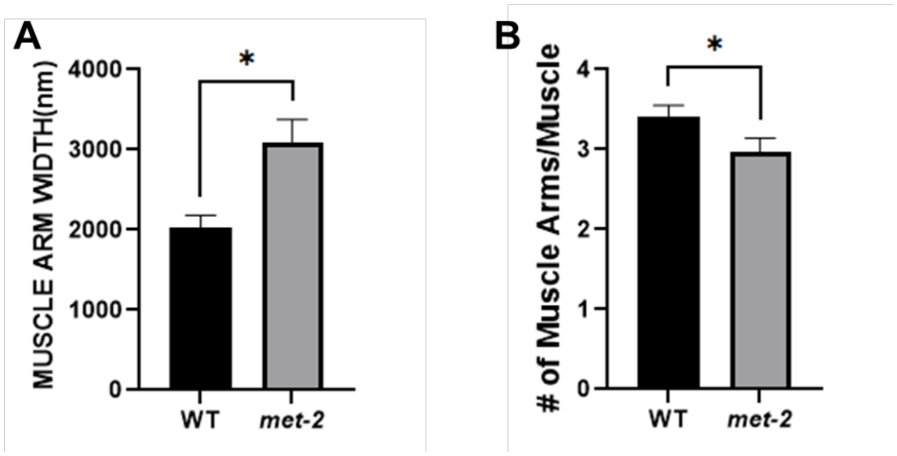

Figure 10: Loss of *met-2* causes muscle arm defects. (A) *met-2* mutant animals (gray $p < 0.05$) exhibit significantly wider muscle arms compared to WT animals (black). (B) WT animals (black $p < 0.05$) have more muscle arms per muscle compared to *met-2* mutant animals (gray). n=228 WT, n=194 *met-2* (muscle arm width). n=67 WT, n=65 *met-2* (# of muscle arms/muscle)

To confirm her results and increase the size of the data set, I also imaged wild type and *met-2* mutant animals using LSM880 confocal microscopy. After analyzing my data, I reanalyzed Erin's images and compared the muscle arms of the *met-2* mutant and wild type animals from my images to Erin's. The results showed no significant difference; thus, I combined all data for a more robust analysis (Figure 11). Like previously seen, I observed that *met-2* mutants had significantly wider muscle arms compared to wild type (Figure 12). I also compared the number of muscle arms per muscle of wild type and *met-2* mutant animals and with the larger sample size the results showed that the wild-type and *met-2* animals had the same number of muscle arms. (Figure 13).

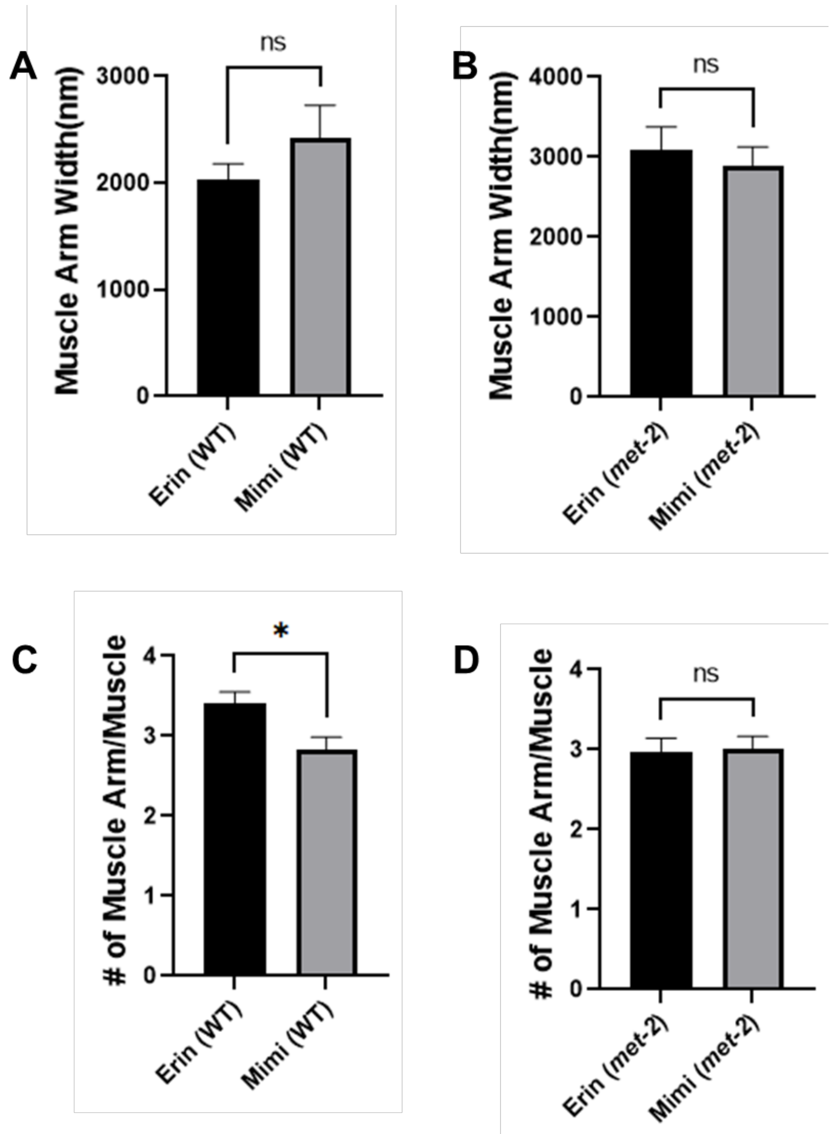

Figure 11: Comparison Data of Muscle Arm Width and Number of Muscle Arms in WT and *met-2*. Comparison data does not show a significant difference in muscle arm width between WT(A) and *met-2* (B). My data shows fewer number of muscle arms in WT compared to Erin's WT data ($p < 0.05$) (C). Comparison data does not show a significant difference in the number of muscle arms in *met-2* (D). n=228 Erin (WT), n=112 Mimi (WT), n=194 Erin (*met-2*), n=251 Mimi (*met-2*) (muscle arm width). n=67 Erin (WT), n=41 Mimi (WT), n=65 Erin (*met-2*), n=83 Mimi (*met-2*) (# of muscle arms/muscle).

Further, I analyzed all my images and Erin's images, taking into account whether the muscle arms were dorsal or ventral. After analyzing the aggregated data from my data set and Erin's data set the results showed that *met-2* mutant animals ($p < 0.01$) exhibited wider muscle arms compared to wildtype animals combined (dorsal and ventral) but no significant difference was observed in muscle arm width when separating the data into dorsal or ventral muscle arms (Figure 12). *met-2* mutants showed no significant difference in the number of muscle arms per muscle compared to wild type in the combined data and dorsal muscle arms alone. However, the ventral muscle arms showed an increase in the number of muscle arms per muscle in wild type compared to the *met-2* mutant (Figure 13).

While imaging, I observed that some of the muscle arms start migrating from the muscle at one point of origin then develop extra arms that branch out of the original muscle arm. Both branches migrate and innervate the nerve cord at two different points. To determine if *met-2* mutation displays this phenotype, I decided to analyze all of the images for branched muscle arms in wild type and *met-2* mutant animals. The results showed that *met-2* mutants had a significant increase in the percentage of branched muscle arms compared to wild type in the combined data and dorsal muscle arms alone but there was no significant difference in the percentage of branched muscle arms between *met-2* mutants and wild type on the ventral side (Figure 14).

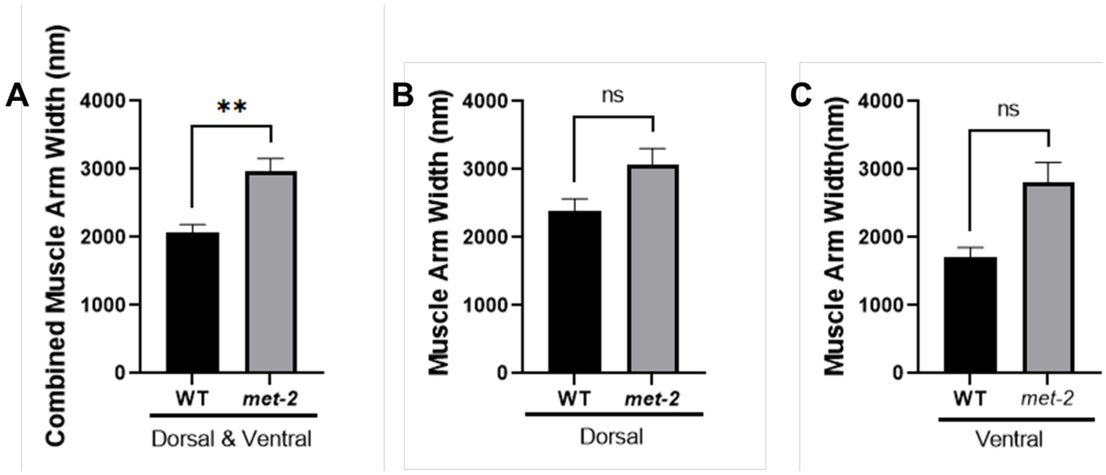

Figure 12: Loss of *met-2* Causes Wider Muscle Arms. The *met-2* mutant (gray $p < 0.01$) has significant wider muscle arms compared to WT (black) overall (A). The *met-2* mutant (gray, ns) does not show any significant difference in muscle arm width dorsally (B) and ventrally (C). n=345 WT, n=447 *met-2* (combined). n=183 WT, n=280 *met-2* (Dorsal). n=162 WT, n=167 *met-2* (Ventral).

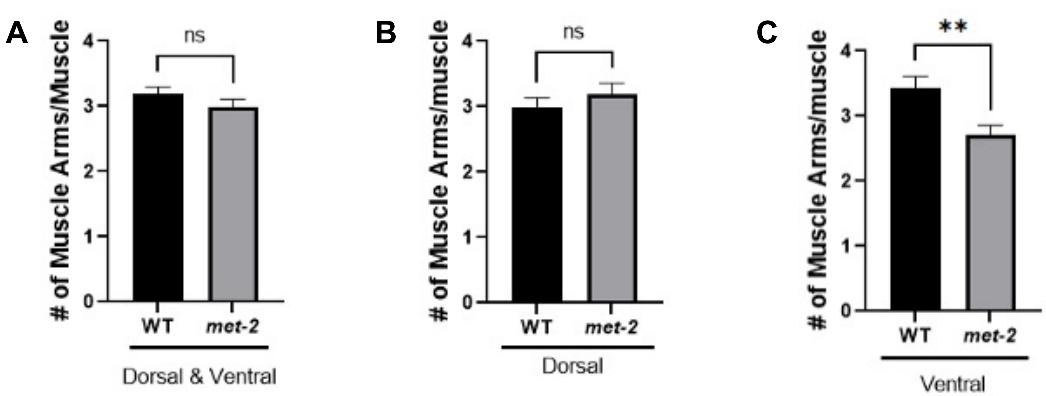

Figure 13: Loss of *met-2* Does Not Affect Number of Muscle Arms. The *met-2* mutant (gray, ns) has no significant difference in number of muscle arms compared to WT (black) overall (A) and dorsally (B). An increase in number of muscle arms is observed in WT (black) compared to the *met-2* mutant (gray $p < 0.01$) ventrally (C). n=108 WT, n=148 *met-2* (combined). n=61 WT, n=86 *met-2* (Dorsal). n=47 WT, n=62 *met-2* (Ventral).

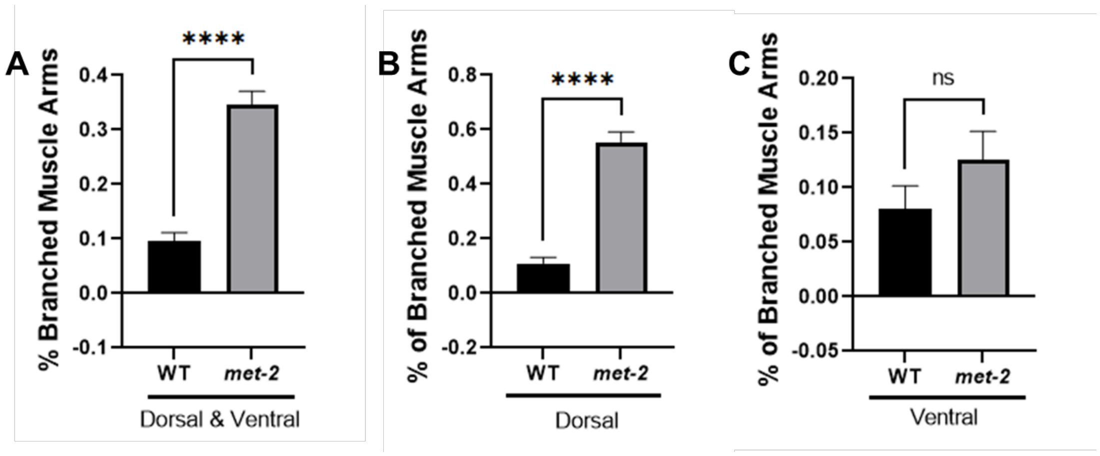

Figure 14: Loss of *met-2* Causes Branched Muscle Arms. The *met-2* mutant (gray $p<0.0001$) shows significant percentage increase in the number of branched muscle arms compared to WT (black) overall (A) and dorsally (B). *met-2* mutant (gray, ns) shows no significant percentage difference compared to WT (black) ventrally (C). n=345 WT, n=342 *met-2* (combined). n=183 WT, n=175 *met-2* (Dorsal). n=162 WT, n=167 *met-2* (Ventral).

3.2 Analysis of Muscle Arms in MET-2 Mutant and NLS::MET-2 Animals

In *C. elegans*, *met-2* has been shown to function in the nucleus and not in the cytoplasm, but the results of the levamisole assays suggested that MET-2 may have a cytoplasmic role. So, to determine if cytoplasmic MET-2 is necessary for muscle arm development or if it has any effect on muscle arm phenotype, I used the LSM880 confocal microscope to determine if sequestration of MET-2 in the nucleus affected muscle arm morphology. I imaged the strain containing nuclear-localized MET-2, *trIs30;* NLS::FLAG::MET-2 and compared it to the *trls30* wild type and *met-2* mutants that were used as controls.

After analyzing my images, in the combined data (dorsal and ventral) *met-2* mutants displayed wider muscle arms ($p < 0.05$) compared to WT and significantly wider muscle arms compared to NLS::MET-2 ($p < 0.0001$). On the dorsal side, HMT mutant only exhibited wider muscle arms ($p < 0.01$) compared to NLS::MET-2 but not WT. The ventral muscle arms showed no significant difference in muscle arm width for all three strains (Figure 16). There was no significant difference overall observed in the number of muscle arm per muscle in wild type, *met-2* mutant and NLS::MET-2 but the ventral side displayed an increase in the number of muscle arms per muscle in wildtype ($p < 0.05$) compared to the *met-2* mutant (Figure 17). The *met-2* mutants also showed a significant increase in the percentage of branched muscle arms compared to wildtype and NLS::MET-2 in the combined data and on the dorsal side (Figure 18). Overall the NLS::MET-2 animals were not significantly different from wildtype in any of the parameters.

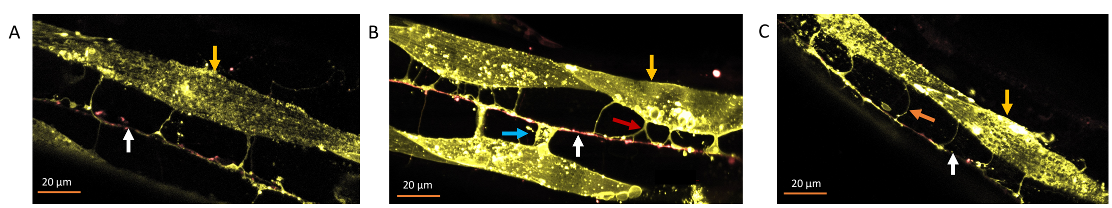

Figure 15: Visualization of Muscle Arms in WT, *met-2* and NLS::MET-2 Animals. Confocal images of muscle arms migrating from muscles (yellow arrows) innervating the dorsal nerve cord (white arrows). (A) WT animal exhibits thin muscle arms, (B) HMT mutant exhibits wider muscle arms (blue arrows) and branching in some of the muscle arms (red arrow) (B). (C)Thin muscle arms (orange arrow) observed in NLS::MET-2 animal.

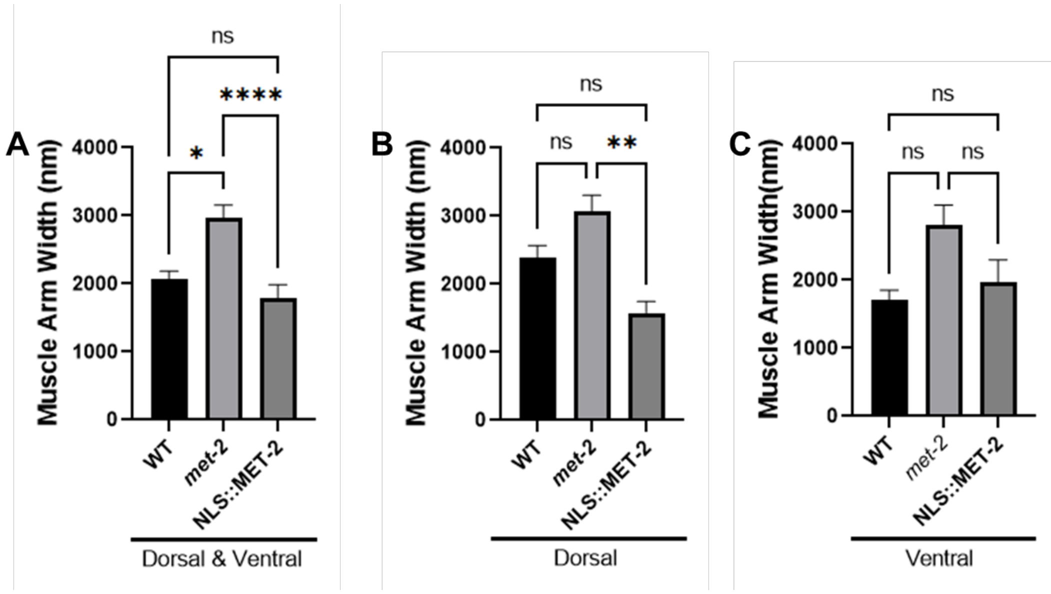

Figure 16: Muscle Arm Width in WT, *met-2*, and NLS::MET-2 Animals. *met-2* mutants show wider muscle arms (gray p< 0.05) compared to WT (black) and NLS::MET-2 (dark gray p< 0.0001). (B) Dorsally, HMT mutant only exhibited wider muscle arms (gray p< 0.01) compared to NLS::MET-2 (dark gray) but not WT (black). (C) Ventrally, no significant difference. n=345 WT, n=447 *met-2*, n=129 NLS::MET-2(combined). n=183 WT, n=280 *met-2,* n=58 NLS::MET-2 (Dorsal). n=162 WT, n=167 *met-2,* n=71 NLS::MET-2 (Ventral).

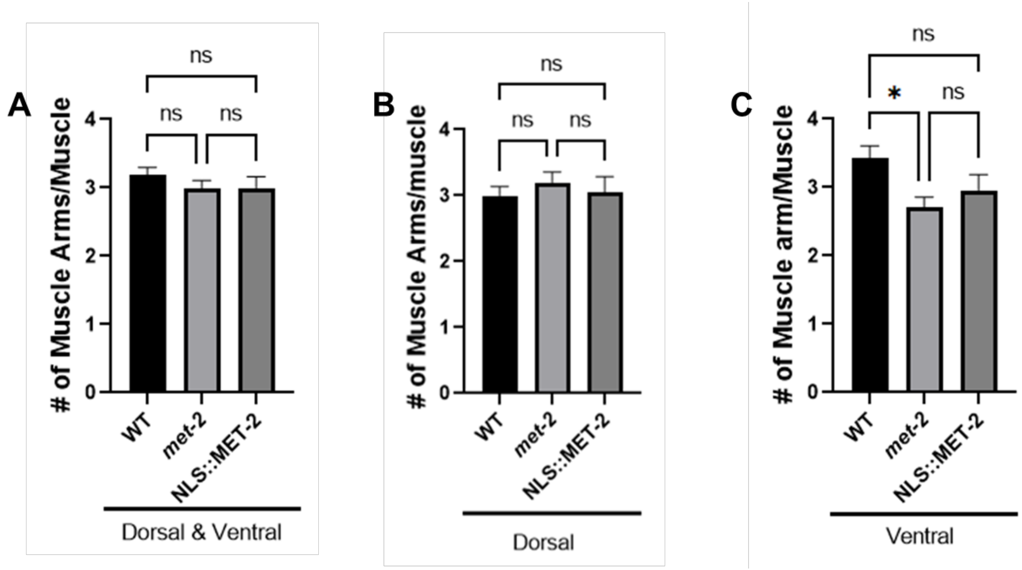

Figure 17: Number of Muscle Arm Per Muscle in WT, *met-2* and NLS::MET-2. Ventrally, an increased number of muscle arms per muscle was observed in the WT (black $p< 0.05$) compared to the *met-2* mutant (gray) otherwise, no significant difference in number of muscle arm per muscle. n=108 WT, n=148 *met-2*, n=43 NLS::MET-2(combined). n=61 WT, n=86 *met-2,* n=19 NLS::MET-2 (Dorsal). n=47 WT, n=62 *met-2,* n=24 NLS::MET-2 (Ventral).

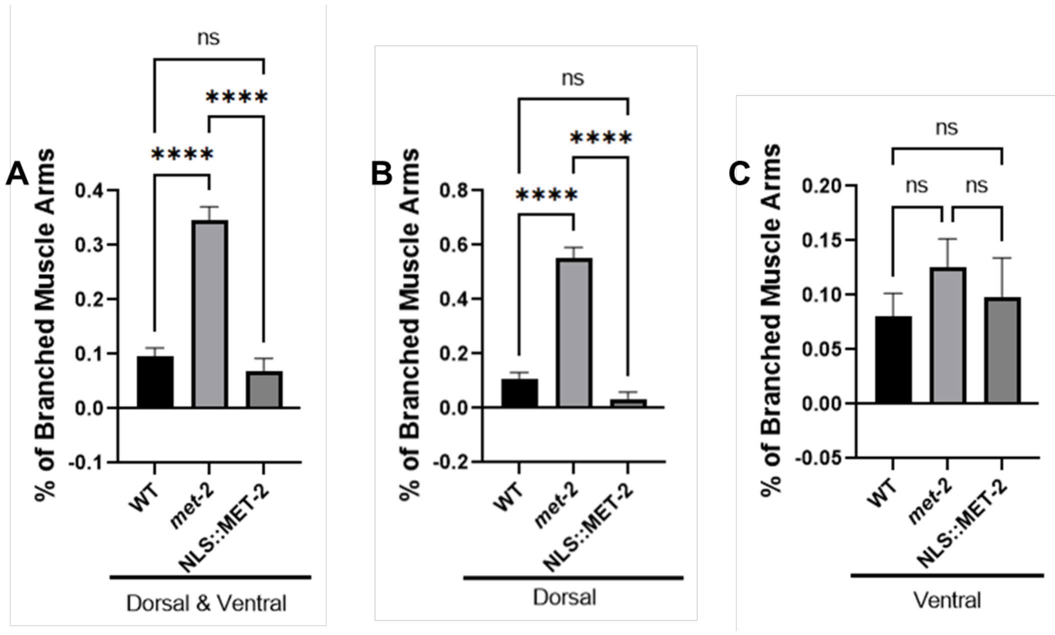

Figure 18: Branched Muscle Arms in WT, *met-2*, and NLS::MET-2 Animals. (A, B) The *met-2* mutant ($p< 0.0001$) has a significantly higher percentage of branched muscle arms compared to WT (black) and NLS::MET-2 (dark gray) combined and dorsally. (C) Ventrally, there is no significant difference in the percentage of branched muscle arm for all three strains. n=345 WT, n=342 *met-2*, n=129 NLS::MET-2(combined). n=183 WT, n=175 *met-2,* n=58 NLS::MET-2 (Dorsal). n=162 WT, n=167 *met-2,* n=71 NLS::MET-2 (Ventral).

3.3 MET-2::GFP Localization in the Cytoplasm of the Muscle

Since previous results suggest that MET-2 could play a cytoplasmic role, I needed to determine if MET-2 is indeed in the cytoplasm of the muscle. As a control, I started by using the LSM880 confocal microscope to image multiple embryos and germ cells of a strain that had GFP inserted with CRISPR on the C- terminus of *met-2*. The images showed MET-2::GFP localized in the nuclei of the germ cells and embryo. Next, I imaged adult animals using the LSM880 confocal microscope, but the images did not show any significant signal above the background. I then imaged rolled adult animals using the more sensitive Dragonfly spinning disk and super resolution microscope. From the images I was able to identify MET-2:: GFP in a striated pattern in the cytoplasm of the muscle (Figure 19).

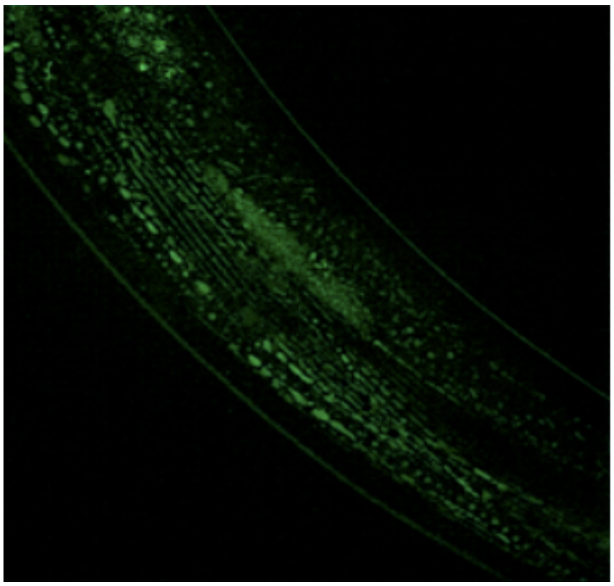

Figure 19: MET-2::GFP is cytoplasmic in the body wall muscles.

Chapter 4

DISCUSSION

Histone methyltransferases are associated with specific gene silencing or activation via methylation of histones in the nucleus. In *C. elegans,* MET-2 is a histone methyltransferase that is required for the placement and accumulation of the repressive histone modification H3K9me2 in the adult germ line (Greer et. al, 2014). When our collaborators in the Mango lab performed a pull down with a Kme antibody, they identified that LEV-11(tropomyosin) in wild type, but not *met-2* mutant animals. This was surprising because LEV-11 only functions in the cytoplasm. Our lab decided to investigate if *met-2* mutant and *lev-11* knockdown animals had similar phenotypes. The hypersensitivity of both *met-2* mutant and *lev-11* knockdown animals in the levamisole time course assay showed that loss of these genes caused the same phenotype, having an impact on postsynaptic function. To test if MET-2 had a cytoplasmic role, another levamisole time course assay was performed using MET-2 with a nuclear localization sequence inserted using CRISPR (NLS::MET-2). These animals with functional MET-2 in their nucleus still showed hypersensitivity to levamisole which indicated that MET-2 plays a cytoplasmic role.

The purpose of my work was to determine if cytoplasmic MET-2 is necessary for proper muscle arm morphology as well as determine if MET-2::GFP localizes in the cytoplasm of the muscle. Dixon and Roy showed that *lev-11* (tropomyosin) knockdown animals exhibit significantly wider and fewer muscle arms compared to wild type animals (Dixon and Roy 2005). So, to explore if the loss of *met-2* also disrupts muscle arms, I performed extensive confocal imaging on wild-type and *met-2* mutant animals. *met-2* mutants exhibited significantly wider muscle arm width compered to wild type when comparing the entire data set. When looking only at muscle arms on the dorsal side or ventral side there was no difference in muscle arm width. This could be the result of a difference in sample size since the sample size imaged for the ventral and dorsal side was less than the overall combined data. While there was no difference in the number of muscle arms per muscle when looking at the combined data, we did see that wild type exhibited a significantly higher number of muscle arms per muscle on the ventral side. This could be because of specific muscle arms analyzed in the different body wall muscle (BWM) quadrants. The number of muscle arms that extend from different BWMs within the same quadrant varies (Dixon and Roy 2005) so this may account for a possible source of error since we did not control for this on either the dorsal or ventral side. Finally, I saw an increase in muscle arm branching in the *met-2* mutant, suggesting that loss of *met-2* could be contributing to a higher number of muscle arms becoming branched. Overall, the results support the conclusion that MET-2 is necessary for muscle arm morphology but not formation.

Given that the NLS::MET-2 displayed the same levamisole hypersensitivity phenotype as *met-2* mutant we hypothesized that it will also exhibit wide muscle arms like the *met-2* mutants. To investigate the muscle arm morphology of animals with MET-2 sequestered to the nucleus, I imaged the strain containing nuclear-localized MET-2, NLS::MET-2. We were surprised to see that their muscle arm width was more similar to the wild type and not the *met-2* mutant. The *met-2* mutant animals showed significantly wider muscle arms than NLS::MET-2, which was not significantly different than the wild type. These results suggest that MET-2 may act in the nucleus to affect the transcription of genes required to regulate the width of muscle arms.

Although certain proteins like MADD-2 have been known to work in concert with transmembrane receptor, UNC-40, and Rho GEF UNC-73 to guide muscle arms to the midline (Alexander et al, 2010) in *C. elegans,* not much is known about what causes branching in muscle arms. While analyzing the images, I noticed that some of the muscle arms had branching, and I decided to measure and analyze the branched muscle arms to determine if the loss of *met-2* in the cytoplasm was responsible for this strange morphology. There was a significant increase in branched muscle arms observed in *met-2* mutants in the combined (dorsal and ventral) and dorsal side. However, in the NLS::MET-2, the percentage of branched muscle arms was relatively equal to wild type and significantly lower than *met-2* mutant. This suggests that loss of *met-2* may contribute to muscle arm branching by affecting transcription.

My results with NLS::MET-2 are consistent with MET-2 not affecting muscle arm morphology via a cytoplasmic role. However, another possibility is that a single nuclear localization sequence is not sufficient to sequester MET-2 in the nucleus. To test this we will have to insert GFP at the C-terminus of MET-2 in the NLS::MET-2 animals. We will then image the strain to determine if MET-2 is actually effectively localized to the nucleus. Alternatively, even if NLS::MET-2 is sequestered in the nucleus, MET-2 could still play a role in the cytoplasm, just not impact muscle arms.

My other aim in this study was to determine if MET-2 was localized in the cytoplasm of the muscle and to do this I imaged a strain that had GFP inserted with CRISPR on the C-terminus of *met-2*. Using the Andor Dragonfly spinning disk and super resolution microscope I visualized MET-2::GFP in a striated pattern in the muscles. I did not see it in muscle arms, but I may need to look at more animals. Alternatively, MET-2::GFP may not be in muscle arms which would explain why NLS::MET-2 looked like WT.

This localization pattern of MET-2::GFP is similar to what has been seen for mitochondrial proteins. The muscle mitochondria are arranged along the sarcomere of the muscle in a parallel pattern and can be visualized by red fluorescent protein (RFP) tagged at the N terminus of the translocase of outer mitochondrial membrane TOMM-20 (Wei and Ruvkun, 2020). I have created a strain that expresses both MET-2::GFP and TOMM-20::DsRed2 to determine if there is any colocalization between the two fluorescent proteins and will image this strain on the Dragonfly. In yeast, tubular mitochondria have been observed to colocalize with actin filaments (Greg *et al*, 1997). The deletion of TPM1, the gene encoding for tropomyosin 1 in yeast causes loss of actin cables and leads to defects in mitochondrial morphology, organization, and motility patterns (Simon *et al*, 1997). So, altered mitochondrial morphology could result to reduced ATP production and lead to levamisole hypersensitivity observed in the *met-2* mutant. Lewis et al hypothesized that levamisole paralysis occurs because of ATP depletion and through metabolic exhaustion (Lewis et al, 1980). A levamisole time course assay performed on the knockdowns of 14 genes identified in a genome wide RNAi screen required for ATP synthesis exhibited levamisole hypersensitivity phenotype (Chaya *et al*, 2021). If MET-2 localizes at or near mitochondria, we will look at mitochondrial morphology in the *met-2* mutant and NLS::MET-2 animals to determine if it may be responsible for the levamisole hypersensitivity phenotype.

In conclusion, we were able to determine that loss of *met-2* leads to defects in muscle arm morphology. Although my results with NLS::MET-2 did not support my hypothesis, it remains unclear whether this is because MET-2 nuclear function impacts muscle arms or if NLS::MET-2 is not actually sequestered in the nucleus. MET-2::GFP was also visualized in the muscle. In the future we will determine if cytoplasmic MET-2 localizes near the mitochondria and if it is required for proper mitochondria morphology. We only explored the cytoplasmic role of MET-2 but for future directions we can explore other HMTs that may have cytoplasmic functions.

REFERENCES

Altun Z. F., and D. H. Hall, 2005 Worm Atlas Hermaphrodite Handbook - Muscle System - Introduction. Worm Atlas. https://doi.org/10.3908/wormatlas.1.6

Barnes, D. E., Watabe, E., Ono, K., Kwak, E., Kuroyanagi, H., & Ono, S. (2018). Tropomyosin isoforms differentially affect muscle contractility in the head and body regions of the nematode Caenorhabditis elegans. Molecular biology of the cell, 29(9), 1075–1088. https://doi.org/10.1091/mbc.E17-03-0152

Black JC, Van Rechem C, Whetstine JR. Histone lysine methylation dynamics: establishment, regulation, and biological impact. Mol Cell (2012) 48(4):491–507.10.1016/j.molcel.2012.11.006

Branscombe, T. L., Frankel, A., Lee, J. H., Cook, J. R., Yang, Z., Pestka, S., & Clarke, S. (2001). PRMT5 (Janus kinase-binding protein 1) catalyzes the formation of symmetric dimethylarginine residues in proteins. The Journal of biological chemistry, 276(35), 32971–32976. https://doi.org/10.1074/jbc.M105412200

Carballido-López R. (2006). The bacterial actin-like cytoskeleton. *Microbiology and molecular biology reviews: MMBR*, *70*(4), 888–909. https://doi.org/10.1128/MMBR.00014-06

Casciello, F., Windloch, K., Gannon, F., & Lee, J. S. (2015). Functional Role of G9a Histone Methyltransferase in Cancer. Frontiers in immunology, 6, 487. https://doi.org/10.3389/fimmu.2015.00487

Chaya, T., Patel, S., Smith, E. M., Lam, A., Miller, E. N., Clupper, M., Kervin, K., & Tanis, J. E. (2021). A C. elegans genome-wide RNAi screen for altered levamisole sensitivity identifies genes required for muscle function. *G3 (Bethesda, Md.)*, *11*(4), jkab047. https://doi.org/10.1093/g3journal/jkab047

Checchi, P. M., & Engebrecht, J. (2011). Caenorhabditis elegans histone methyltransferase MET-2 shields the male X chromosome from checkpoint machinery and mediates meiotic sex chromosome inactivation. *PLoS genetics*, *7*(9), e1002267. https://doi.org/10.1371/journal.pgen.1002267

Cho, A., Kato, M., Whitwam, T., Kim, J. H., & Montell, D. J. (2016). An Atypical Tropomyosin in Drosophila with Intermediate filament-like Properties. Cell reports, 16(4), 928–938. https://doi.org/10.1016/j.celrep.2016.06.054

Cooper GM. The Cell: A Molecular Approach. 2nd edition. Sunderland (MA): Sinauer Associates; 2000. Actin, Myosin, and Cell Movement. Available from: https://www.ncbi.nlm.nih.gov/books/NBK9961/

Corsi, A. K., Wightman, B., & Chalfie, M. 2015. A Transparent Window into Biology: A Primer on Caenorhabditis elegans. Genetics, 200(2), 387–407. https://doi.org/10.1534/genetics.115.176099

Dominguez, R., & Holmes, K. C. (2011). Actin structure and function. *Annual review of biophysics*, *40*, 169–186. https://doi.org/10.1146/annurev-biophys-042910-155359

Dixon, S. J., & Roy, P. J. 2005. Muscle arm development in Caenorhabditis elegans. Development (Cambridge, England), 132(13), 3079–3092. https://doi.org/10.1242/dev.01883

Dixon, S. J., Alexander, M., Fernandes, R., Ricker, N., & Roy, P. J. (2006). FGF negatively regulates muscle membrane extension in Caenorhabditis elegans. Development (Cambridge, England), 133(7), 1263–1275. https://doi.org/10.1242/dev.02300

Dos Remedios, C. G., Chhabra, D., Kekic, M., Dedova, I. V., Tsubakihara, M., Berry, D. A., & Nosworthy, N. J. (2003). Actin binding proteins: regulation of cytoskeletal microfilaments. *Physiological reviews*, *83*(2), 433–473. https://doi.org/10.1152/physrev.00026.2002

EM Jorgensen, ML Nonet - seminars in DEVELOPMENTAL BIOLOGY, 1995

Eric L. Greer, Sara E. Beese-Sims, Emily Brookes, Ruggero Spadafora, Yun Zhu, Scott B. Rothbart, David Aristizábal-Corrales, Shuzhen Chen, Aimee I. Badeaux, Qiuye Jin, Wei Wang, Brian D. Strahl, Monica P. Colaiácovo, Yang Shi, A Histone Methylation Network Regulates Transgenerational Epigenetic Memory in C. elegans, Cell Reports,Volume 7, Issue 1,2014, Pages 113-126, ISSN 2211-1247.https://doi.org/10.1016/j.celrep.2014.02.044.

Frézal, L., & Félix, M. A. 2015. C. elegans outside the Petri dish. eLife, 4, e05849. https://doi.org/10.7554/eLife.05849

Gallant, C., Appel, S., Graceffa, P., Leavis, P., Lin, J. J., Gunning, P. W., Schevzov, G., Chaponnier, C., DeGnore, J., Lehman, W., & Morgan, K. G. (2011). Tropomyosin variants describe distinct functional subcellular domains in differentiated vascular smooth muscle cells. American journal of physiology. Cell physiology, 300(6), C1356–C1365. https://doi.org/10.1152/ajpcell.00450.2010

Gateva, G., Kremneva, E., Reindl, T., Kotila, T., Kogan, K., Gressin, L., Gunning, P. W., Manstein, D. J., Michelot, A., & Lappalainen, P. (2017). Tropomyosin Isoforms Specify Functionally Distinct Actin Filament Populations In Vitro. Current biology: CB, 27(5), 705–713. https://doi.org/10.1016/j.cub.2017.01.018

Goins, L. M., & Mullins, R. D. (2015). A novel tropomyosin isoform functions at the mitotic spindle and Golgi in Drosophila. Molecular biology of the cell, 26(13), 2491–2504. https://doi.org/10.1091/mbc.E14-12-1619

Greg J. Hermann, Edward J. King, Janet M. Shaw; The Yeast Gene, *MDM20,* Is Necessary for Mitochondrial Inheritance and Organization of the Actin Cytoskeleton. *J Cell Biol* 7 April 1997; 137 (1): 141–153.
doi: https://doi.org/10.1083/jcb.137.1.141

Gruninger, T. R., Gualberto, D. G., LeBoeuf, B., & Garcia, L. R. (2006). Integration of male mating and feeding behaviors in Caenorhabditis elegans. The Journal of neuroscience: the official journal of the Society for Neuroscience, 26(1), 169–179. https://doi.org/10.1523/JNEUROSCI.3364-05.2006

Gunning, P. W., Schevzov, G., Kee, A. J., & Hardeman, E. C. (2005). Tropomyosin isoforms: divining rods for actin cytoskeleton function. Trends in cell biology, 15(6), 333–341. https://doi.org/10.1016/j.tcb.2005.04.007

https://doi.org/10.1016/B978-0-7020-6697-9.00001-7

Jambhekar, A., Dhall, A., & Shi, Y. (2019). Roles and regulation of histone methylation in animal development. Nature reviews. Molecular cell biology, 20(10), 625–641. https://doi.org/10.1038/s41580-019-0151-1

James A Lewis, C-H Wu, Howard Berg, Joseph H Levine, THE GENETICS OF LEVAMISOLE RESISTANCE IN THE NEMATODE *CAENORHABDITIS ELEGANS*, *Genetics*, Volume 95, Issue 4, 1 August 1980, Pages 905928, https://doi.org/10.1093/genetics/95.4.905

Kerr, S. C., Ruppersburg, C. C., Francis, J. W., & Katz, D. J. (2014). SPR-5 and MET-2 function cooperatively to reestablish an epigenetic ground state during passage through the germ line. *Proceedings of the National Academy of Sciences of the United States of America*, *111*(26), 9509–9514. https://doi.org/10.1073/pnas.1321843111

Levitan, Irwin; Kaczmarek, Leonard (August 19, 2015). "Intercellular communication". The Neuron: Cell and Molecular Biology (4th ed.). New York, NY: Oxford University Press. pp. 153–328. ISBN 978-0199773893.

Lewis, J. A., Wu, C. H., Berg, H., & Levine, J. H. (1980). The genetics of levamisole resistance in the nematode Caenorhabditis elegans. *Genetics*, *95*(4), 905–928. https://doi.org/10.1093/genetics/95.4.905

Manstein, D. J., & Mulvihill, D. P. (2016). Tropomyosin-Mediated Regulation of Cytoplasmic Myosins. Traffic (Copenhagen, Denmark), 17(8), 872–877. https://doi.org/10.1111/tra.12399

May;171(1):1-7. DOI: 10.1016/j.molbiopara.2009.12.007. PMID: 20064566; PMCID: PMC2838958

McIntire, S. L., Jorgensen, E., Kaplan, J., & Horvitz, H. R. (1993). The GABAergic nervous system of Caenorhabditis elegans. Nature, 364(6435), 337–341. https://doi.org/10.1038/364337a0

Ono, K., & Ono, S. (2004). Tropomyosin and troponin are required for ovarian contraction in the Caenorhabditis elegans reproductive system. Molecular biology of the cell, 15(6), 2782–2793. https://doi.org/10.1091/mbc.e04-03-0179

Pathak, A., Chatterjee, N., & Sinha, S. 2020. Developmental trajectory of Caenorhabditis elegans nervous system governs its structural organization. PLoS computational biology, 16(1), e1007602. https://doi.org/10.1371/journal.pcbi.1007602

Peggy Hung, Maureen Lai, Sukhvir Toor & Bowen Zhao (2017). Comparison of wild-type and unc-2 mutant Caenorhabditis elegans egg-laying rates. The expedition, vol. 6, Issue 1,2016.

Pollard, T. D., & Cooper, J. A. (2009). Actin, a central player in cell shape and movement. *Science (New York, N.Y.)*, *326*(5957), 1208–1212. https://doi.org/10.1126/science.1175862

Raizen DM, Zimmerman JE, Maycock MH, Ta UD, You YJ, Sundaram MV, Pack AI

Nature. 2008 Jan 31; 451(7178):569-72.

Richmond, J. E., & Jorgensen, E. M. (1999). One GABA and two acetylcholine receptors function at the C. elegans neuromuscular junction. Nature neuroscience, 2(9), 791–797. https://doi.org/10.1038/12160

Robertson AP, Clark CL, Martin RJ. Levamisole and ryanodine receptors. I: A contraction study in Ascaris suum. Molecular and Biochemical Parasitology. 2010

Rygiel, K (August 2016). "The ageing neuromuscular system and sarcopenia: a mitochondrial perspective". J. Physiol. **594** (16): 4499–4512. doi:10.1113/JP271212. PMC 4983621. PMID 26921061.

Simon, V. R., Karmon, S. L., & Pon, L. A. (1997). Mitochondrial inheritance: cell cycle and actin cable dependence of polarized mitochondrial movements in Saccharomyces cerevisiae. *Cell motility and the cytoskeleton*, *37*(3), 199–210. https://doi.org/10.1002/(SICI)1097-0169(1997)37:3<199::AID-CM2>3.0.CO;2-2

Sulston, J. E., and Horvitz, H. R. (1977). Post-embryonic cell lineages of the nematode, Caenorhabditis elegans. Dev. Biol. 56,110-156.

Velarde, N., Gunsalus, K. C., & Piano, F. (2007). Diverse roles of actin in C. elegans early embryogenesis. *BMC developmental biology*, *7*, 142. https://doi.org/10.1186/1471-213X-7-142

Wei, W., & Ruvkun, G. (2020). Lysosomal activity regulates *Caenorhabditis elegans* mitochondrial dynamics through vitamin B12 metabolism. *Proceedings of the National Academy of Sciences of the United States of America*, *117*(33), 19970–19981. https://doi.org/10.1073/pnas.2008021117

Wood, A., & Shilatifard, A. (2004). Posttranslational modifications of histones by methylation. Advances in protein chemistry, 67, 201–222. https://doi.org/10.1016/S0065-3233(04)67008-2

Yang, C., Zhang, J., Ma, Y., Wu, C., Cui, W., & Wang, L. (2020). Histone methyltransferase and drug resistance in cancers. Journal of experimental & clinical cancer research: CR, 39(1), 173. https://doi.org/10.1186/s13046-020-01682-z

zeiss-campus.magnet.fsu.edu/articles/spectralimaging/introduction.html

Zhen, M., & Samuel, A. D. (2015). C. elegans locomotion: small circuits, complex functions. Current opinion in neurobiology, 33, 117–126. https://doi.org/10.1016/j.conb.2015.03.009